


Novel ultra-hard hexacarbon allotropes from first principles

Samir F. Matar^{1,§,*} and Vladimir L. Solozhenko²

¹ Lebanese German University (LGU), Sahel-Alma, Jounieh, Lebanon.

 <https://orcid.org/0000-0001-5419-358X>

² LSPM–CNRS, Université Sorbonne Paris Nord, 93430 Villetaneuse, France.

 <https://orcid.org/0000-0002-0881-9761>

[§] Former DRI–CNRS senior researcher at the University of Bordeaux, ICMCB–CNRS, France

*Corresponding author email: s.matar@lgu.edu.lb and abouliess@gmail.com

Abstract

Novel ultra-hard carbon allotropes are proposed based on crystal chemistry rationale and geometry optimization onto ground state structures. Like diamond, new orthorhombic, tetragonal, and trigonal C₆ are identified as cohesive networks of C₄ tetrahedra illustrated by charge density projections exhibiting sp³-like carbon hybridization. The three allotropes are mechanically (elastic constants) and dynamically (phonons) stable. Furthermore, they exhibit thermal properties like those of diamond. The electronic band structures are characteristic of insulators with large band gaps of 4 to 5 eV. From four different models evaluating Vickers hardness new carbon allotropes are identified as ultra-hard with H_V close to 95 GPa.

Keywords: *DFT; crystal chemistry; carbon allotropes; ultra-hard materials, thermal properties, phonons.*

1. Introduction and context

Until very recently diamond was the only material qualified as ultrahard. Despite its unique properties i.e. extreme hardness, elevated thermal conductivity, large band gap, high electron and hole mobility making it suitable for diverse basic research and applications, the reactivity of diamond with oxygen and ferrous metals constitute a drawback. Furthermore, diamond's hardness drastically drops with temperature. As consequence, there is a growing demand for other advanced materials that stimulated the search for novel ultra-hard thermally and chemically stable phases (cf. [1,2-4] and references therein).

In 2009 ultra-hard diamond-like BC_5 was synthesized by Solozhenko *et al.* [5]. This phase corresponds to the ultimate solubility of boron in diamond and possesses Vickers hardness of 71 GPa, unusually high for superhard materials fracture toughness ($\sim 10 \text{ MPa}\cdot\text{m}^{1/2}$), and very high (up to 1900 K) thermal stability which makes it an exceptional superabrasive superior to diamond. Diamond-like BC_5 is metastable phase and can be synthesized only in a narrow temperature range under pressures above 20 GPa which makes its production quite a challenge.

Yao *et al.* attempted revealing thermodynamic stable polymorphs of BC_5 from structural searches combined with first-principles structural optimizations [6]. Besides of tetragonal ($I\bar{4}m2$) polymorph, trigonal ($P3m1$) and triclinic ($P-1$) forms of BC_5 were theoretically predicted. The study revealed mixed stacking of covalent C–C and metallic B–C substructures with an overall metallic system keeping ultra-hard mechanical properties.

In as far as BC_5 can be considered as a B-substituted carbon network, the hypothetic system with full carbon occupancy becomes an extended three-dimensional (3D) carbon, candidate for ultra-hardness. Extended 3D carbon networks have gained interest in view of the challenging question: “*is diamond the hardest material*” as generally admitted? In this context, hexagonal $6H$ carbon ($P6_3/mmc$ space group) was claimed to be harder than diamond [7], and we recently discussed the ultra-hardness of a novel rhombohedral carbon allotrope ($rh-C_4$) [8] which can be considered as an extended hexagonal $h-C_{12}$ lattice presenting mechanical properties like those of diamond (Vickers hardness $H_V \sim 100 \text{ GPa}$).

The present study was carried out within the well-established quantum density functional theory DFT framework [9,10] with the aim to highlight the ultra-hardness along with modern models of novel hexacarbon C_6 structures based on three BC_5 forms. In particular, the mechanical (elastic constants) and dynamical (phonons bands) stabilities of these phases were confirmed. Furthermore, they are identified with thermal properties alike diamond. Orthorhombic, tetragonal, and trigonal C_6 all have energies close to diamond's and are equally characterized by a stacking of $C4$ tetrahedra. The electronic band structures are shown to exhibit insulating behavior like diamond with large gaps close to 5 eV.

2. Computational framework

The search for the ground state structures through geometry optimizations and total energies calculations was performed using the plane-wave Vienna Ab initio Simulation Package (VASP) code [9,10] based on DFT. The projector augmented wave (PAW) method [11,12] was used for the atomic potentials with all valence states, especially in regard of such light element as carbon. DFT exchange-correlation (XC) effects were considered using the generalized gradient approximation (GGA) [14]. For the relaxation of the atoms onto ground state geometry, a conjugate-gradient algorithm [15] was applied. Improved tetrahedron method [16] with corrections according to Methfessel-Paxton scheme [17] was applied for geometry optimization and energy calculations. A special \mathbf{k} -point sampling [18] was applied for approximating the reciprocal space Brillouin-zone (BZ) integrals. For better reliability, the optimization of the structural parameters was carried out along with successive self-consistent cycles with increasing mesh until the forces on atoms were less than 0.02 eV/\AA and the stress components below 0.003 eV/\AA^3 .

Besides the elastic constants calculated to infer the mechanical stabilities and hardness, further calculations of phonon dispersion curves were also carried out to verify the dynamic stability of new carbon allotropes. In the present work, the phonon modes were computed considering the harmonic approximation via finite displacements of the atoms around their equilibrium positions to obtain the forces from the summation over the different configurations. The phonon dispersion curves along the direction of the Brillouin zone are subsequently obtained using "Phonopy" interface code based on Python language [19]. Thermodynamic properties such as the Helmholtz free energy, the heat capacity C_v and the entropy S , were calculated as functions of temperature.

3. Calculations and results

3.1-Energy and crystal symmetry

The novel C_6 structures were derived from the orthorhombic, tetragonal, and trigonal carbon rich BC_5 by selective substitutions of boron by carbon leading to the hexacarbon systems. The structures were then geometry optimized to their respective stress-free ground states. The energy is the prevailing criterion for the first assessment of the new structures. The total energies: E_{total} (eV) and the derived atom-averaged energies E_{atom} are presented in Table 1. Additionally, the results for *rh*- C_4 (*h*- C_{12}) [8] and diamond are given. All atom-averaged values of C_6 structures are found very close to diamond, thus pointing out their stability, at least with respect to diamond.

The C_6 structures are shown in Fig. 1. All three structures exhibit tetrahedral carbon $C4$ (sp^3) featured with four small yellow sticks stemming from each atom. Such tetrahedral shape is well known to be characteristic of diamond and provides a signature for totally covalent 3D carbon.

The crystal data provided in Table 2 present the converged calculated new atomic positions after full unconstrained geometry optimization with successive calculations at increasing precision of \mathbf{k} -mesh in the three respective Brillouin zones. The starting values of the corresponding BC_5 from

Ref. [6] are given in brackets. It can be noticed a clear increase of symmetry upon replacing B by C resulting in remarkable atomic positions and relationships between the atomic coordinates, as highlighted and detailed at the bottom of each part of Table 2. A unique interatomic C–C distance of 1.55 Å characteristic of diamond is found for all C₆ allotropes.

3-2. Charge density 3D projections

Further illustration of “electronic ↔ crystal structure” relationship focusing on the tetrahedral C(sp³)-like carbon as the building unit of the novel allotropes, can be provided by the charge density projections. Fig. 2 shows the charge density volumes (yellow) with perfect sp³ tetrahedral shape around carbon. For the two body-centered orthorhombic (*Imm2*) and body-centered tetragonal (*I4̄m2*) allotropes, the primitive cells with 12 carbon atoms are represented. Due to simple trigonal C₆ the stacking of tetrahedra is most clearly demonstrated among the three projections, with the tetrahedral yellow volumes.

3-3. Mechanical properties

(i) Elastic constants

The investigation of mechanical characteristics was based on the calculations of the elastic properties determined by performing finite distortions of the lattice and deriving the elastic constants from the strain-stress relationship. Most compounds are polycrystalline, and generally considered as randomly oriented single crystalline grains. Consequently, on a large scale, such materials can be considered as statistically isotropic. They are then fully described by bulk (*B*) and shear (*G*) moduli obtained by averaging the single-crystal elastic constants. The method used here is Voigt's [20], based on a uniform strain. The calculated sets of elastic constants are given in Table 3. All values are positive. Their combinations obeying the rules pertaining to the mechanical stability of the phase, and the equations providing the bulk *B_V* and shear *G_V* moduli are as follows [21].

- For the orthorhombic system:

$$C_{ii} \ (i=1, 4, 5, 6) > 0; \ C_{11}C_{22} - C_{12}^2 > 0; \ C_{11}C_{22}C_{33} + 2C_{12}C_{13}C_{23} - C_{11}C_{23}^2 - C_{22}C_{13}^2 - C_{33}C_{12}^2 > 0.$$

$$B_{Voigt}^{orth.} = 1/9 (C_{11} + 2C_{12} + 2C_{13} + C_{22} + 2C_{23} + C_{33})$$

$$G_{Voigt}^{orth.} = 1/15 (C_{11} - C_{12} - C_{13} + C_{22} - C_{23} + C_{33} + 3C_{44} + 3C_{55} + 6C_{44} + 3C_{66})$$

- For the tetragonal system:

$$C_{ii} \ (i=1, 3, 4, 6) > 0; \ C_{11} > C_{12}, \ C_{11} + C_{33} - 2C_{13} > 0; \ \text{and} \ 2C_{11} + C_{33} + 2C_{12} + 4C_{13} > 0.$$

$$B_{Voigt}^{tetr.} = 1/9 (2C_{11} + C_{33} + 2C_{12} + 4C_{13}).$$

$$G_{Voigt}^{tetr.} = 1/15 (2C_{11} + C_{12} + 2C_{33} - 2C_{13} + 6C_{44} + 3C_{66}).$$

- For the hexagonal (trigonal) system:

$$C_{11} > C_{12}, C_{11}C_{33} > C_{13}^2 \text{ and } (C_{11}+C_{12}) C_{33} > 2C_{13}^2$$

$$B_{\text{Voigt}}^{\text{hex.}} = 1/9 \{2(C_{11} + C_{12}) + 4C_{13} + C_{33}\}$$

$$G_{\text{Voigt}}^{\text{hex.}} = 1/30 \{C_{11} + C_{12} + 2C_{33} - 4C_{13} + 12C_{44} + 6(C_{11} - C_{12})\}$$

The calculated values for all three C_6 carbon allotropes in Table 3 exhibit large B_V (> 400 GPa) and G_V (> 500 GPa) values that are comparable with the accepted values for diamond. Such results allow assigning ultra-hard mechanical properties to the novel carbon allotropes and extracting hardness-related properties as developed in the next subsection.

(ii) *Hardness*

Vickers hardness (H_V) was predicted using four pertinent theoretical models of hardness [22-25]. The thermodynamic model [22] is based on thermodynamic properties and crystal structure, while Mazhnik-Oganov [24] and Chen-Niu [25] models use the elastic properties. Lyakhov-Oganov approach [23] considers topology of the crystal structure, strength of covalent bonding, degree of ionicity and directionality. The fracture toughness (K_{Ic}) was evaluated within the Mazhnik-Oganov model [24].

The results are summarized in Tables 4 and 5. Table 4 presents Vickers hardness and bulk moduli (B_0) calculated in the framework of the thermodynamic model of hardness. Table 5 presents hardness calculated using four different theoretical models and other mechanical properties such as shear modulus (G), Young's modulus (E), the Poisson's ratio (ν) and fracture toughness (K_{Ic}).

A slightly lower hardness of h - C_6 and rh - C_3 compared to diamond (both cubic and hexagonal) is observed for both models (Table 4). On the other hand, hardness of these phases is much higher than hardness of the vast majority of recently predicted carbon allotropes (C_{14} , C_{16} , C_{24} , C_{36} , etc.) [29-33].

A good agreement of the bulk moduli of three new C_6 allotropes and rh - C_4 [8] estimated using the thermodynamic model (B_0) and calculated from the set of elastic constants (B_V) is observed. For all three phases K_{Ic} is almost twice higher than the 2.8 MPa·m^{1/2} value for single-crystal cubic BN [34] and close to the experimental value of diamond fracture toughness (5 MPa·m^{1/2}) [35].

Thus, all three C_6 allotropes have exceptional mechanical properties among all recently proposed carbon allotropes [29-33] and thus can be considered as prospective ultra-hard materials [1].

3-4. *Dynamical stabilities from the phonons.*

Beside structural stability criteria obeyed by all three new carbon phases through the positive magnitudes of the elastic constants and their combinations, we computed the phonon modes.

Phonons, quanta of vibrations, have their energy quantized - just like photons - through the Planck constant 'h' used in its reduced form \hbar ($\hbar = h/2\pi$) giving with the wave number ω the energy: $E = \hbar\omega$.

Following the method presented in Section 2, the obtained phonon band structures for three new C_6 phases are shown in Fig. 3. In each panel along the horizontal direction, the bands run along the main lines of orthorhombic (Fig. 3a), tetragonal (Fig. 3b) and hexagonal (Fig. 3c) Brillouin zones. Along the vertical direction the frequencies are given in units of terahertz (THz). Since no negative frequency magnitudes are observed, all three C_6 structures can be considered as dynamically stable. There are 3N-3 optical modes at high energy and 3 acoustic modes. The two body-centered orthorhombic ($Imm2$) and tetragonal ($I\bar{4}m2$) allotropes were accounted for using primitive cells with 12 carbon atoms, whence the larger number of bands versus trigonal C_6 (Fig. 3c). The acoustic modes start from zero energy ($\omega = 0$) at the Γ point, center of the Brillouin Zone, up to a few Terahertz. They correspond to the lattice rigid translation modes of the crystal (two transverse and one longitudinal). Then 30 bands are expected in Figs. 3a and 3b, and 15 bands in Fig. 3c. But knowing that the higher the symmetry, the more dispersion curves showing degeneracy are found for a given frequency, an apparent reduction in the number of dispersion curves is observed. In the three panels the energy range is the same for all three phases, i.e. from 0 to 40 THz, stressing furthermore their similitude with the magnitude observed for diamond by Raman spectroscopy: $\omega \sim 40$ THz [36].

3-5. Thermal properties.

After the phonon band structures, the thermal properties such as free energy, entropy and heat capacity C_v were calculated using the statistical thermodynamic expressions from the phonon frequencies on a high precision sampling mesh in the BZ (cf. the textbook by Dove on 'Lattice Dynamics' [37]). All three allotropes were found to present similar curves. Fig. 4 shows the temperature change of entropy and heat capacity at constant volume, and the Helmholtz free energy: $F = U-TS$ where U stands for the internal energy and S for entropy. The plots are shown in two panels for diamond and trigonal C_6 as representative of all hexacarbon allotropes.

For the two phases, the free energy decreases with temperature as expected from the equation above because S increases with T almost linearly as it can be seen in both panels. In Fig. 4a, the entropy S and the heat capacity are close to zero up to 100 K. Above 100 K, S increases continuously and almost linearly up to the highest temperatures. For the heat capacity curves, a validation of the evolution of C_v was found from experimental data on diamond's heat capacity up to high temperatures obtained by Victor back in 1962 [38]. The discrete experimental points obtained from 300K up to 1000K by steps of 100K are plotted as open symbols on the calculated curve (green). An excellent agreement can be observed, except for the last two points at the highest temperature. While supporting our calculated results, this feature is interesting and may raise the remark as to the stability of the measurements and of diamond sample at such high temperatures.

Fig. 4b shows results for trigonal hexacarbon showing similarity with diamond. For the sake of comparison, the experimental points from [38] were reported. Up to 700 K, the heat capacity of C₆ is higher than that of diamond, while at higher temperatures the curve follows the experimental points for diamond with the same feature (as in Fig. 4a) for the last two points departing from the curve.

3.6 Electronic band structures.

Fig. 5 shows the electronic band structures for three new C₆ allotropes obtained using the all-electrons DFT-based augmented spherical method (ASW) [39]. The energy level along the vertical line is with respect to the top of the valence band (VB), E_V. The VB is largely separated from the empty conduction band CB by a large band gap amounting to ~5 eV. Such insulating electronic character resembles diamond. A few features relevant to the nature of the band gap can be observed such as the indirect in orthorhombic and hexagonal (trigonal) C₆, like in diamond but identified as indirect between Γ_{VB} and Γ_{CB} in tetragonal C₆ allotrope.

Acknowledgments: Computational facilities from the University of Bordeaux and from the Lebanese German University are gratefully acknowledged.

Author Contributions: Samir F. Matar: Structure conceptualization. Software. Computations. Vladimir L. Solozhenko: Hardness evaluation. Expertise in hard materials.

Funding: This research received no external funding.

Data Availability Statement: Data supporting reported results including CIF files can be made available on demand.

Conflicts of Interest. The authors declare no conflict of interest.

REFERENCES

- [1] V.L. Solozhenko, Y. Le Godec, A hunt for ultrahard materials. *J. Appl. Phys.* **126**, 230401 (2019).
- [2] V.L. Solozhenko, High-pressure synthesis of novel superhard phases. in: "*Comprehensive Hard Materials*" (eds. V.K. Sarin and C.E. Nebel), Elsevier, 2014, pp. 641-652.
- [3] Y. Le Godec, A. Courac, V. L. Solozhenko, High-pressure synthesis of superhard and ultrahard materials. *J. Appl. Phys.* **126**, 151102 (2019).
- [4] S.F. Matar, V.L. Solozhenko, Crystal chemistry and ab initio prediction of ultrahard rhombohedral B₂N₂ and BC₂N. *Solid State Sci.* **118**, 106667 (2021).
- [5] V.L. Solozhenko, O.O. Kurakevych, D. Andrault, Y. Le Godec, M. Mezouar, Ultimate metastable solubility of boron in diamond: Synthesis of superhard diamondlike BC₅. *Phys. Rev. Lett.* **102**, 015506 (2009).
- [6] Y. Yao, J.S. Tse, D.D. Klug, Crystal and electronic structure of superhard BC₅: First-principles structural optimizations. *Phys. Rev. B* **80**, 094106 (2009).
- [7] F. Gao, J. Zhanga, Z. Lia, Origin of ultrahardness of 6H diamond: harder than cubic diamond. *RSC Adv.* **4**, 32345-32347 (2014).
- [8] S.F. Matar, V.L. Solozhenko, Ultra-hard rhombohedral carbon from crystal chemistry rationale and first principles. *J. Solid State Chem.* **302**, 122354 (2021).
- [9] P. Hohenberg, W. Kohn, Inhomogeneous electron gas. *Phys. Rev. B* **136**, 864-871 (1964).
- [10] W. Kohn, L.J. Sham, Self-consistent equations including exchange and correlation effects. *Phys. Rev. A* **140**, 1133-1138 (1965).
- [11] G. Kresse, J. Furthmüller, Efficient iterative schemes for ab initio total-energy calculations using a plane-wave basis set. *Phys. Rev. B* **54**, 11169 (1996).
- [12] G. Kresse, J. Joubert, From ultrasoft pseudopotentials to the projector augmented wave. *Phys. Rev. B* **59**, 1758-1775 (1999).
- [13] P.E. Blöchl, Projector augmented wave method. *Phys. Rev. B* **50**, 17953-17979 (1994).
- [14] J. Perdew, K. Burke, M. Ernzerhof, The Generalized Gradient Approximation made simple. *Phys. Rev. Lett.* **77**, 3865-3868 (1996).
- [15] W.H. Press, B.P. Flannery, S.A. Teukolsky, W.T. Vetterling, Numerical Recipes, 2nd ed. Cambridge University Press: New York, USA, 1986.
- [16] P.E. Blöchl, O. Jepsen, O.K. Anderson, Improved tetrahedron method for Brillouin-zone integrations. *Phys. Rev. B* **49**, 16223-16233 (1994).
- [17] M. Methfessel, A.T. Paxton, High-precision sampling for Brillouin-zone integration in metals. *Phys. Rev. B* **40**, 3616-3621(1989).

- [18] H.J. Monkhorst, J.D. Pack, Special k-points for Brillouin Zone integration. *Phys. Rev. B* **13**, 5188-5192 (1976).
- [19] A. Togo, I. Tanaka, First principles phonon calculations in materials science. *Scr. Mater.* **108**, 1-5 (2015).
- [20] W. Voigt, Über die Beziehung zwischen den beiden Elasticitätsconstanten isotroper Körper. *Annal. Phys.* **274**, 573-587 (1889).
- [21] D.C. Wallace, Thermodynamics of crystals. New York, USA: John Wiley and Sons; 1972.
- [22] V.A. Mukhanov, O.O. Kurakevych, V.L. Solozhenko, The interrelation between hardness and compressibility of substances and their structure and thermodynamic properties. *J. Superhard Mater.*, **30**, 368-378 (2008).
- [23] A.O. Lyakhov, A.R. Oganov, Evolutionary search for superhard materials: Methodology and applications to forms of carbon and TiO₂. *Phys. Rev. B* **84**, 092103 (2011).
- [24] E. Mazhnik, A.R. Oganov, A model of hardness and fracture toughness of solids. *J. Appl. Phys.*, **126**, 125109 (2019).
- [25] X-Q.Chen, H. Niu, D. Li, Y. Li, Modeling hardness of polycrystalline materials and bulk metallic glasses. *Intermetallics*, **19**, 1275-1281 (2011).
- [26] P.D. Ownby, X. Yang, J. Liu, Calculated X-ray diffraction data for diamond polytypes. *J. Am. Ceram. Soc.* **75**, 1876-1883 (1992).
- [27] N. Bindzus, T. Straasø, N. Wahlberg, J. Becker, L. Bjerg, N. Lock, A.-C. Dippel, B.B. Iversen Experimental determination of core electron deformation in diamond. *Acta Cryst. A* **70**, 39-48 (2014).
- [28] V.V. Brazhkin, V.L. Solozhenko, Myths about new ultrahard phases: Why materials that are significantly superior to diamond in elastic moduli and hardness are impossible. *J. Appl. Phys.* **125**, 130901 (2019).
- [29] D. D. Pang, X.Q. Huang, H.Y. Xue, C. Zhang, Z.L. Lv, M.Y. Duan, Properties of a predicted tetragonal carbon allotrope: first principles study. *Diam. Relat. Mater.* **82**, 50-55 (2018).
- [30] W. Zhang, C. Chai, Q. Fan, Y. Song, Y. Yang, Metallic and semiconducting carbon allotropes comprising of pentalene skeletons. *Diam. Relat. Mater.* **109**, 108063 (2020).
- [31] X. Yang, C. Lv, S. Liu, J. Zang, J. Qin, M. Du, D. Yang, X. Li, B. Liu, C.-X. Shan, Orthorhombic C₁₄ carbon: A novel superhard sp³ carbon allotrope. *Carbon* **156**, 309-312(2020).
- [32] Q. Fan, H. Liu, L. Jiang, X. Yu, W. Zhang, S. Yun, Two orthorhombic superhard carbon allotropes: C₁₆ and C₂₄. *Diam. Relat. Mater.* **116**, 108426 (2021).
- [33] Q. Fan, H. Liu, R. Yang, X. Yu, W. Zhang, S. Yun, An orthorhombic superhard carbon allotrope: Pmma C₂₄. *J. Solid State Chem.* **300**, 122260 (2021).

- [34] V.L. Solozhenko, S.N. Dub, N.N. Novikov, Mechanical properties of cubic BC₂N, a new superhard phase. *Diam. Relat. Mater.* **10**, 2228-2231 (2001).
- [35] N.V. Novikov, S.N. Dub, Fracture toughness of diamond single crystals. *J. Hard Mater.* **2**, 3-11 (1991).
- [36] R.S. Krishnan, Raman spectrum of diamond. *Nature* **155**, 171 (1945).
- [37] M.T. Dove, Introduction to lattice dynamics, Cambridge University Press, 1993.
- [38] A.C. Victor, Heat capacity of diamond at high temperatures, *J. Chem. Phys.* **36** (1962) 1903-1911.
- [39] V. Eyert, Basic notions and applications of the augmented spherical wave method. *Int. J. Quantum Chem.* **77**, 1007-1031 (2000).

Table 1 Total and atom averaged energies of different carbon allotropes considered in present work. Energies are in eV units, Z is number of formula units.

Carbon phase	Space group / N°	E_{total}	E/atom	Z
C ₆ (orthorhombic)	<i>Imm2</i> (N° 44)	-109.14	-9.095	2
C ₆ (tetragonal)	$\bar{I}4m2$ (N° 119)	-109.08	-9.090	2
C ₆ (trigonal)	<i>P3m1</i> (N° 156)	-54.57	-9.095	1
C ₁₂ (<i>rh-C₄</i>) [8]	$R\bar{3}m$ (N° 166)	-109.08	-9.090	1
C ₈ (diamond)	<i>Fd\bar{3}m</i> (N° 227)	-72.72	-9.090	4

Table 2 Crystal parameters from DFT calculation of the hexacarbon C₆ structures. Values in brackets are from the corresponding BC₅ forms [6].

a) Orthorhombic C₆, space group *Imm2* (N° 44). (Fig. 1a).

$a = 7.579 \text{ \AA}$; $b = 2.527$; $c = 3.574 \text{ \AA}$. ($Z=2$)

Atom	Wyckoff	x	y	z
C1	2 <i>b</i>	½	0.0	*0.042(0.023)
C2	4 <i>c</i>	1/6 (0.1725)	0.50	*0.292 (0.2835)
C3	4 <i>c</i>	1/6 (0.1686)	0.0	**0.042 (0.0419)
C4	2 <i>a</i>	0.0	0.0	**0.792 (0.826)

$d(\text{C-C}) = 1.55 \text{ \AA}$.

* $0.292 - 0.042 = \frac{1}{4}$

** $0.792 - 0.042 = \frac{3}{4}$

b) Tetragonal C₆, space group $\bar{I}4m2$ (N° 119). (Fig. 1b).

$a = b = 2.519 \text{ \AA}$; $c = 10.690 \text{ \AA}$. ($Z=2$)

Atom	Wyckoff	x	y	z
C1	2 <i>d</i>	0.50	0.0	¼
C2	4 <i>e</i>	0.0	0.0	1/6 (0.1568)
C3	2 <i>b</i>	0.0	0.0	0.50
C4	4 <i>f</i>	0.0	0.50	1/12 (0.0805)

$d(\text{C-C}) = 1.55 \text{ \AA}$.

c) Trigonal C₆, space group *P3m1* (N° 156). (Fig. 1c).

$a = b = 2.521 \text{ \AA}$; $c = 6.180 \text{ \AA}$. ($Z= 1$).

Atom	Wyckoff	x	y	z
C1	1 <i>a</i>	0.0	0.0	0.0 (0.0069)
C2	1 <i>a</i>	0.0	0.0	¼ (0.2598)
C3	1 <i>b</i>	1/3	2/3	1/3 (0.3386)
C4	1 <i>b</i>	1/3	2/3	*0.584(0.581)
C5	1 <i>c</i>	2/3	1/3	2/3 (0.5818)
C5	1 <i>c</i>	2/3	1/3	*0.917(0.664)

$d(\text{C-C}) = 1.55 \text{ \AA}$.

*0.917 = $\frac{1}{3} + 0.584$

Table 3 Elastic constants C_{ij} and Voigt values of bulk (B_V) and shear (G_V) moduli of new carbon allotropes (all values are in GPa).

	C_{11}/C_{22}	C_{12}	C_{13}/C_{23}	C_{33}	C_{44}	C_{55}	C_{66}	B_V	G_V
$C_6 (Imm2)$	1204/1206	43	148/149	1101	476	570	580	465	536
$C_6 (\bar{I}4m2)$	1172/1173	28	134/134	1069	465	437	570	438	502
$C_6 (P3m1)$	1171	99	63	1205	536	501	–	444	542

Table 4 Vickers hardness (H_V) and bulk moduli (B_0) of carbon allotropes calculated in the framework of the thermodynamic model of hardness*

	Space group	a (Å)	b (Å)	c (Å)	ρ (g/cm ³)	H_V (GPa)	B_0 (GPa)
C ₆ (#44)	$Imm2$	7.5799	2.5266	3.5740	3.4967	97	440
C ₆ (#119)	$\bar{I}4m2$	2.5187	2.5187	10.6900	3.5293	98	445
C ₆ (#156)	$P3m1$	2.5214	2.5214	6.1800	3.5172	97	443
<i>rh</i> -C ₄ [8]	$R\bar{3}m$	2.5004	2.5004	12.210	3.6204	100	456
Lonsdaleite	$P63/mmc$	2.5221 [†]	2.5221 [†]	4.1186 [†]	3.5164	97	443
Diamond	$Fd\bar{3}m$	3.5666 [‡]	–	–	3.5169	98	445 [§]

* Ref. 22

† Ref. 26

‡ Ref. 27

§ Ref. 28

Table 5 Mechanical properties of carbon allotropes: Vickers hardness (H_V), bulk modulus (B), shear modulus (G), Young's modulus (E), Poisson's ratio (ν) and fracture toughness (K_{Ic})

	H_V				B		G_V	E^{**}	ν^{**}	K_{Ic}^{\ddagger}
	T [*]	LO [†]	MO [‡]	CN [§]	B_0^*	B_V				
	GPa									
C_6 ($Imm2$)	97	89	101	90	440	465	536	1162	0.084	6.8
C_6 ($I\bar{4}m2$)	98	90	95	86	445	438	502	1090	0.085	6.1
C_6 ($P3m1$)	97	90	103	97	443	444	542	1156	0.066	6.5
$rh-C_4$ [8]	100	93 ^{††}	105	97	456	458	552	1181	0.070	6.7
Lonsdaleite	97	90	99	94	443	432	521	1115	0.070	6.2
Diamond	98	90	100	93	445 ^{††}		530 ^{††}	1138	0.074	6.4

* Thermodynamic model [22]

† Lyakhov-Oganov model [23]

‡ Mazhnik-Oganov model [24]

§ Chen-Niu model [25]

** E and ν values calculated using isotropic approximation

†† Calculated in present work

‡‡ Ref. 28

FIGURES

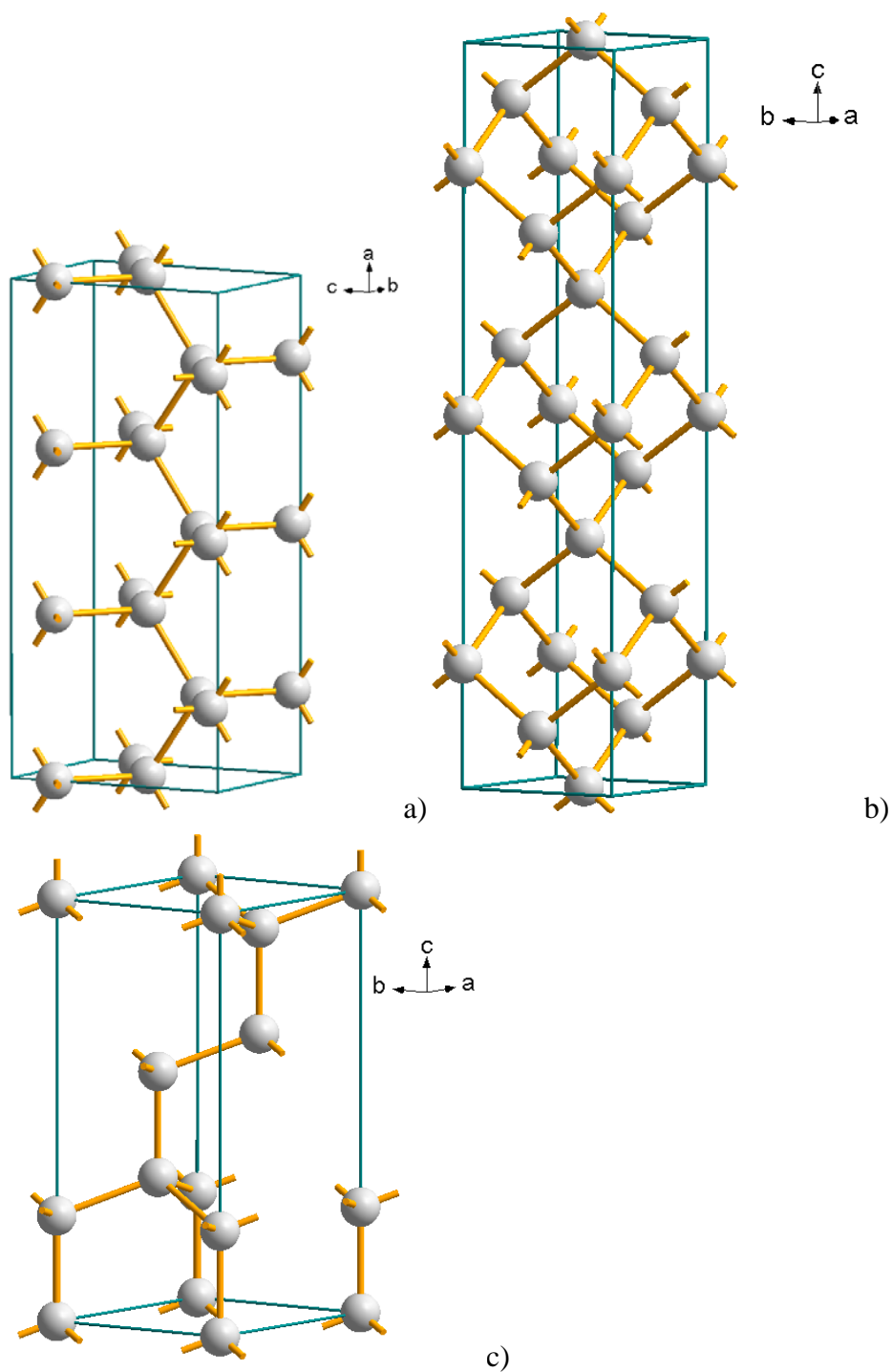


Fig. 1 Structure sketches of three novel C_6 allotropes: a) orthorhombic ($Imm2$); b) tetragonal ($I\bar{4}m2$); c) trigonal ($P3m1$). The tetrahedral coordination is seen with the yellow-orange sticks on each grey sphere carbon atoms.

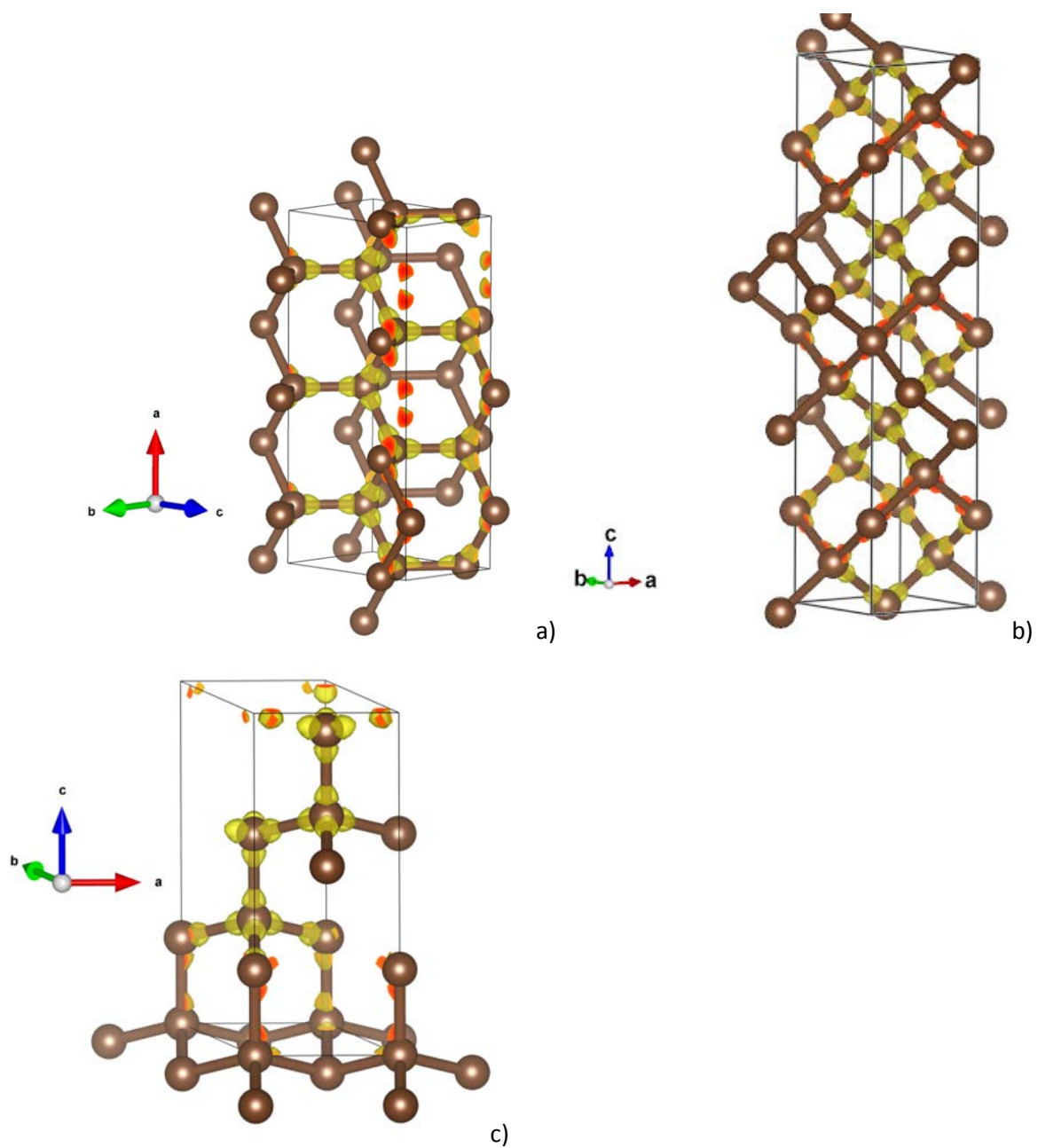


Fig. 2 Charge density yellow volumes around carbon atoms shows tetrahedral sp^3 -like shapes in a) C_6 in simple orthorhombic cell (i.e. C_{12}); b) C_6 in simple tetragonal cell (i.e. C_{12}); and c) trigonal C_6 .

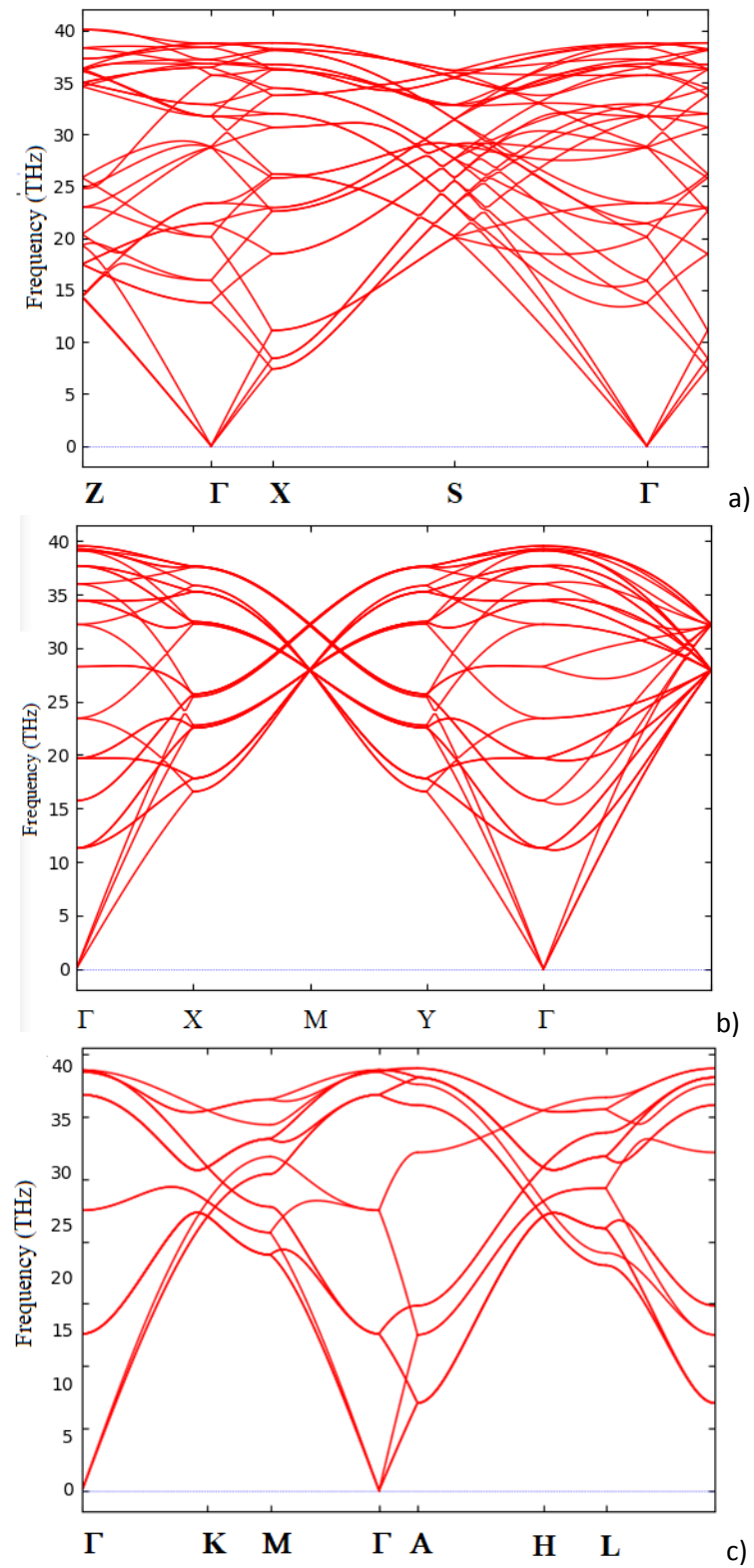
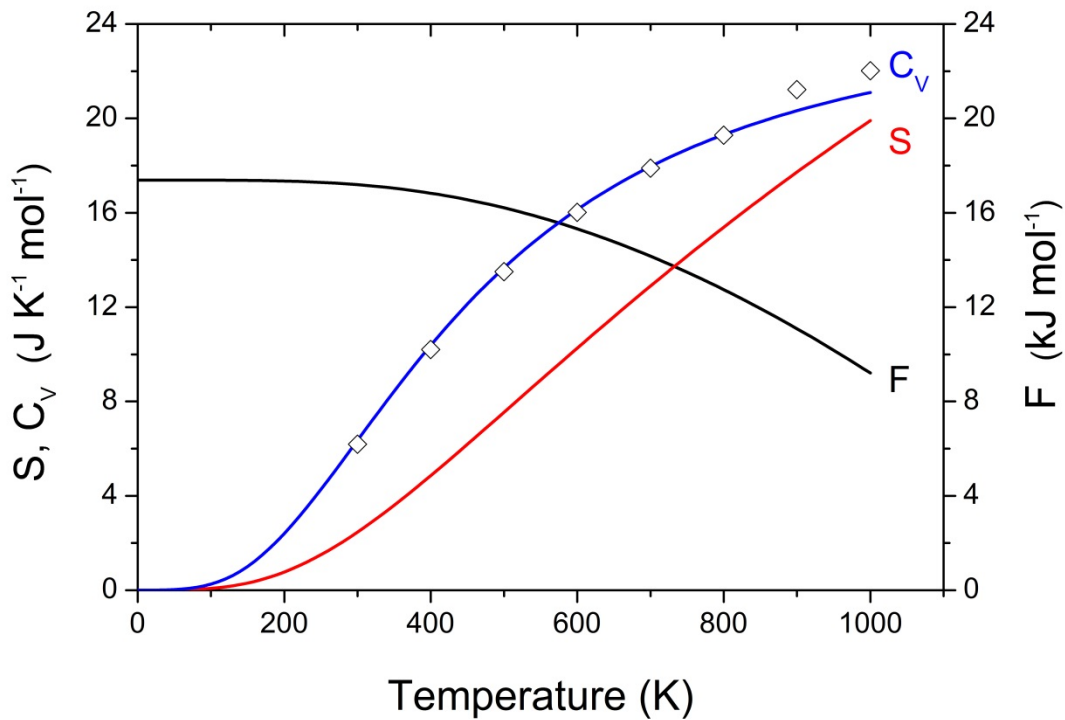
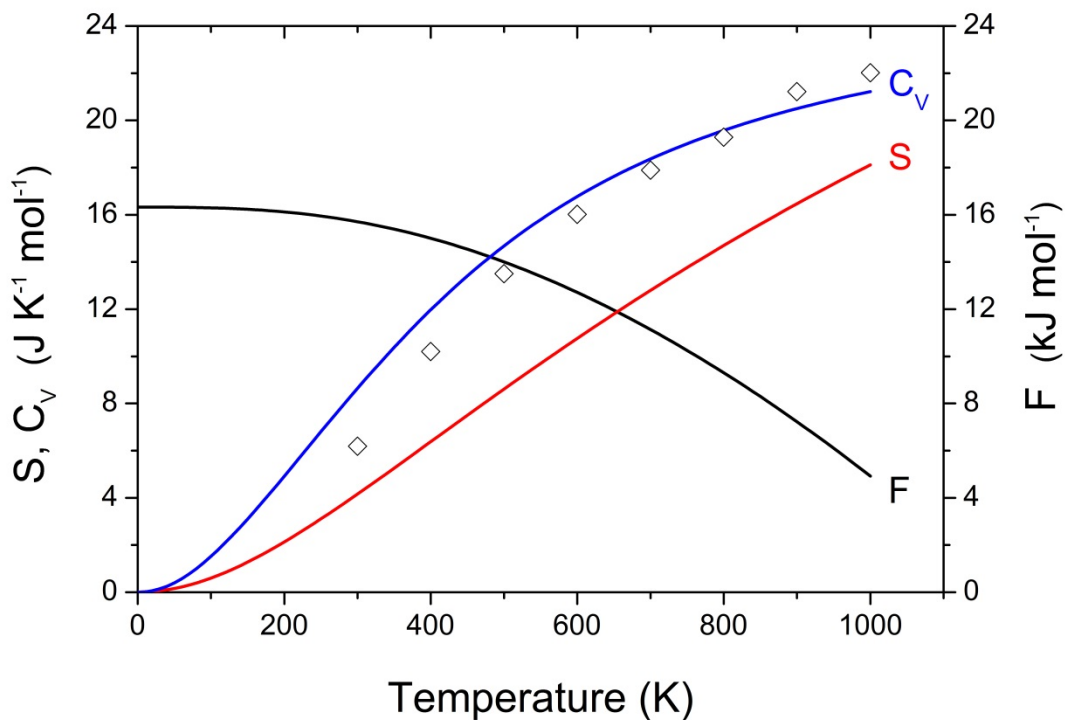


Fig. 3 Phonon band structures along the lines of the different Brillouin zones (along horizontal direction): a) orthorhombic C_6 , b) tetragonal C_6 , c) trigonal C_6 .



a)



b)

Fig. 4 Thermal properties (free energy F, entropy S and specific heat C_V at constant volume) as functions of temperature: a) diamond; the experimental C_V values from Ref. [38] are shown as open symbols; b) trigonal C_6 ; the results are shown as representative of hexacarbon allotropes.

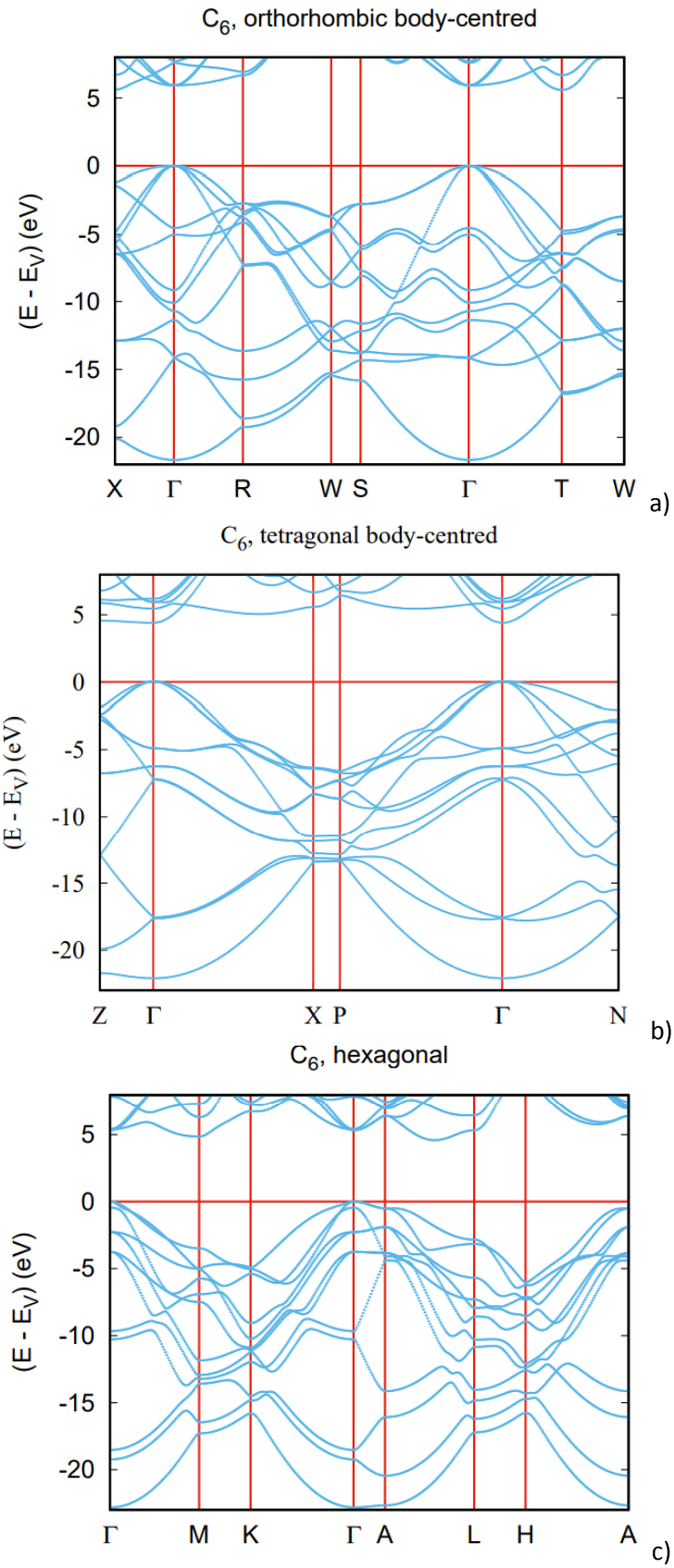


Fig. 5 C₆ allotropes. Electronic band structures exhibiting large band gap like diamond.